Immunity

Article

Cell PRESS

Essential Role of Ubiquitin and TSG101 Protein in Formation and Function of the Central Supramolecular Activation Cluster

Santosha Vardhana,[1] Kaushik Choudhuri,[1] Rajat Varma,[1,2] and Michael L. Dustin[1,*]

[1]Program in Molecular Pathogenesis, Helen L. and Martin S. Kimmel Center for Biology and Medicine of the Skirball Institute of Biomolecular Medicine, and the Department of Pathology, New York University School of Medicine, 540 First Avenue, New York, NY 10016, USA
[2]Current address: NIAID/ LCMI, Bldg 4, Room 431, 4 Center Drive, Bethesda, MD 20892, USA
*Correspondence: dustin@saturn.med.nyu.edu
DOI 10.1016/j.immuni.2010.04.005

SUMMARY

Agonist MHC-peptide complexes in the immunological synapse (IS) signal through T cell receptor (TCR) microclusters (MCs) that converge into a central supramolecular activation cluster (cSMAC). The determinants and function of the cSMAC remain unknown. We demonstrate an essential role for ubiquitin (Ub) and TSG101, but less so for HRS, in signal processing events at the cSMAC. Using siRNA in primary T cells, we show that Ub recognition by TSG101 is required for cSMAC formation, TCR MC signal termination, TCR downregulation, and segregation of TCR-MHC-peptide from PKC-θ-enriched signaling complexes. Weak agonist MHC-peptide induced CD80-dependent TCR MCs that dissociated in the center of the IS without recruiting TSG101. These results support TSG101-dependent recognition of CD80-independent TCR MCs as a molecular checkpoint for TCR downregulation.

INTRODUCTION

Complex signal integration in cells involves responses to diverse stimuli that often utilize overlapping signal transduction machinery. Appropriate responses to such stimuli may benefit from spatial segregation of ligand-receptor interactions. In T cells, immunological synapses (ISs) are specialized cell-cell junctions that combine cell polarization and positional stability with spatial segregation of interacting elements (Dustin, 2002; Dustin et al., 1998; Monks et al., 1998). IS formation is critical for signal integration, as well as coordination of migration, directed secretion, asymmetric cell division, and differentiation (Davis et al., 2007; Dustin, 2008; Huppa and Davis, 2003; Krogsgaard et al., 2003). In CD4+ T cells, the IS is composed of three primary subdomains: a central supramolecular activation cluster (cSMAC) rich in proximal signaling components such as T cell receptor (TCR)-major histocompatibility complex (MHC)-peptide and PKC-θ kinase, a peripheral supramolecular activation cluster (pSMAC) dominated by intercellular adhesion molecule-1 (ICAM-1)-lymphocyte function associated-1 (LFA-1) interactions, and a distal supramolecular activation cluster (dSMAC) rich in dynamic actin (Grakoui et al., 1999; Monks et al., 1998). The cSMAC is generated and maintained by microclusters (MCs) of 10–20 TCRs that continuously form in an actin-dependent manner in the dSMAC but that become actin independent as they translocate to the IS center and fuse to form the cSMAC (Krummel et al., 2000; Varma et al., 2006; Yokosuka et al., 2005). TCR MCs are the sites of signal initiation based on recruitment and phosphorylation of the signaling molecules Lck, ZAP-70, and LAT, as well as SLP-76 and Grb-2 recruitment (Bunnell et al., 2002; Campi et al., 2005; Huse et al., 2007; Yokosuka et al., 2005). In contrast, the cSMAC has 1/20 amount of tyrosine phosphorylation compared with MCs and cannot independently sustain Ca²⁺ signaling (Campi et al., 2005; Varma et al., 2006). The molecular basis of signaling differences between MCs and the cSMAC is unknown.

Ligand-mediated TCR downregulation occurs via routing of internalized receptors to lysosomes (Valitutti et al., 1997), and enrichment of the cSMAC in multivesicular body (MVB) markers suggests a role for receptor degradation at the cSMAC (Varma et al., 2006). However, not all ligands induce cSMAC formation, and it has recently been proposed that avoidance of cSMAC formation and TCR downregulation may underlie the elevated stimulatory potency of certain weak agonist ligands (Cemerski et al., 2007). TCR degradation may occur via ubiquitin (Ub) recognition based on involvement of ubiquitin ligases such as Cbl-b (Naramura et al., 2002). Degradation of ubiquitinated substrates via MVBs is a stepwise process coordinated by multiple family members of the endosomal sorting complex required for transport (ESCRT) (Williams and Urbé, 2007). There are four ESCRT complexes (0, I, II, and III) with unique roles in signal termination and receptor degradation of epidermal growth factor receptor (EGFR). ESCRT-0 and -I directly recognize Ub (Williams and Urbé, 2007). ESCRT-0 can also associate with ubiquitinated cargo through the Ub interaction motif (UIM) of hepatocyte growth factor-regulated tyrosine kinase substrate (HRS) (Bache et al., 2003b; Hirano et al., 2006) in parallel with inositol-3-phosphate bearing lipids present in endosomes (Raiborg et al., 2001). ESCRT-I recognizes Ub through the ubiquitin E3 variant (UEV) domain of tumor suppressor gene 101 (TSG101) and is required for sorting of EGFR into MVBs (Pornillos et al., 2002; Sundquist et al., 2004; Teo et al., 2004). In the absence of TSG101, both MVB formation and sorting of proteins into MVBs is inhibited, resulting instead in persistent EGFR signaling

(Bache et al., 2006; Doyotte et al., 2005). The specific role of ESCRT complexes in TCR downregulation has not been determined.

Unresolved roles for the cSMAC in promoting proximal signaling still exist, particularly with respect to PKCθ, whose enrichment at the cSMAC has been described (Monks et al., 1998; Monks et al., 1997). Activated PKC-θ leads to downstream activation of NF-κB and AP-1 transcription factors (Isakov and Altman, 2002; Sun et al., 2000). CD28 is dispensable for PKC-θ recruitment to the IS, but is critical for its concentration in the cSMAC (Huang et al., 2002). Recent reports have suggested discrete sites of CD28, PKCθ, and TCR enrichment within the IS (Sims et al., 2007; Tseng et al., 2008; Yokosuka et al., 2008), but the molecular basis for this segregation is as yet unclear. Understanding mechanisms of segregation may provide insight into how cells simultaneously process multiple signals.

To address the role of Ub and ESCRT-mediated Ub recognition in cSMAC formation and function, we have applied siRNA-mediated suppression and high-resolution fluorescence microscopy of IS formed between primary T cells and supported bilayers. We determined that Ub was required for cSMAC formation in the IS in response to agonist MHC-peptide complexes. Ub recognition by ESCRT-I component TSG101, but not ESCRT-0 component HRS, was required for cSMAC formation, TCR MC signal termination, and segregation of TCR-agonist MHCp complexes from PKC-θ-enriched domains within an outer cSMAC subdomain. We also demonstrated that TSG101 was rapidly recruited to the plasma membrane after T cell activation by fluorescence resonance energy transfer. Finally, signaling MCs formed in response to weak agonist ligands remained actin dependent and dissipated at the cSMAC-pSMAC boundary without recruiting ESCRT-I complexes. The IS thus engages in a conditional utilization of ESCRT-I and spatially defined checkpoints to regulate T cell signaling and downregulation.

RESULTS

Ubiquitination Is Required for cSMAC Formation
Prior observations that MVBs are enriched at the cSMAC led us to investigate whether ubiquitination is involved in IS patterning (Varma et al., 2006). Treatment of cells with MG132 inhibits the proteosome, resulting in accumulation of poly-ubiquitinated substrates and depletion of the free ubiquitin pool (Melikova et al., 2006). We therefore incubated MG132-treated AND TCR transgenic (Tg) T cells on supported planar bilayers presenting I-E^k-MCC + ICAM-1. Control treated T cells formed TCR MCs, which accumulated in the cSMAC in response to bilayers presenting agonist MHC-peptide (Figure 1A; Figure S1A and Movie S1 available online). In contrast, we found that MG132-treated T cells were able to efficiently form TCR MCs, but were unable to translocate MCs from the site of formation to the IS center. The amount of TCR accumulating at the interface was increased significantly in the MG132-treated cells (Figure 1B). Furthermore, MG132 treatment significantly impeded termination of TCR signals, given that phosphorylation of peripherally accumulated TCR MCs was 5- to 10-fold higher in MG132 treated T cell IS as compared to control T cell IS (Figures 1A and 1B). Although MG132 treatment may have a number of additional effects, these results suggest that ubiquitination is

required for cSMAC formation and encouraged us to further pursue this line of experimentation.

TSG101 Is Required for cSMAC Formation and MC Dephosphorylation
The suggested role for ubiquitination in cSMAC formation led us to investigate the role of ubiquitin recognizing ESCRT complex components in regulating TCR signaling within the IS. We chose to target HRS and TSG101, the respective critical components of the ESCRT-0 and ESCRT-I complexes with established ubiquitin binding (Figure 1C) (Williams and Urbé, 2007). We developed a procedure to efficiently suppress expression of HRS or TSG101 in 100% of activated AND TCR transgenic (Tg) T cells, by nucleofection of either specific siRNA duplexes or scrambled versions of the same sequence as controls. We were able to reduce HRS and TSG101 expression more than 90% during primary expansion of AND TCR Tg T cells (Figure 1D).

In EGFR systems, ESCRT-0 is initially recruited to ubiquitinated cargo within clathrin-coated pits and is required for efficient receptor degradation (Bache et al., 2003a; Bilodeau et al., 2003; Katzmann et al., 2003). However, HRS knockdown (KD) T cells formed a cSMAC containing dephosphorylated TCR (Figures 1E and 1F). In addition, T cells transfected with GFP-tagged clathrin light chain showed no colocalization of clathrin-coated pits with TCR MCs in the IS (Figure S1B and Movie S2). However, clathrin-coated pits were present in distinct puncta emerging in the IS periphery and accumulated in the IS center (Figure S1B and Movie S2). Furthermore, HRS KD resulted in accumulation of phosphotyrosine in the IS periphery that did not colocalize with TCR (Figures 1E and 1F). This leaves open the possibility that clathrin-HRS might be involved in regulation of downstream signaling complexes that are known to dissociate from TCR MCs and signal independently (Bunnell et al., 2002); however, because this phenotype is distinct from that of MG132 treatment, we did not pursue this further here.

In contrast to HRS, TSG101 KD generated a phenotype more similar to that of MG132 treatment. Control siRNA-treated cells formed TCR MCs, which accumulated in the cSMAC in response to bilayers presenting agonist MHCp. In contrast, TCR MCs failed to translocate to the cSMAC and instead accumulated more peripherally in TSG101 KD T cells (Figure 1G, Figures S1C and S1D, and Movie S3). TSG101 KD resulted in accumulation of phosphorylated TCR MCs in quantities and distribution that were similar to MG132-treated T cell IS (Figures 1G and 1H and Figures S1C and S1D), suggesting that TSG101 translocates ubiquitinated TCR MCs to the cSMAC for dephosphorylation and degradation. The elevated antiphosphotyrosine intensity in TSG101 KD ISs did not correlate directly with the TCR intensity in MCs, but all visible TCR MCs were intensely phosphotyrosine positive, except in rare cases in which TCR MCs penetrated into the IS center. A proportion of the elevated phosphotyrosine signal in TSG101 KD ISs did not colocalize with TCR. This may be due to phosphorylation of small clusters of TCR that are below the limit of detection. Alternatively, they may represent other surface proteins, such as LAT and associated proteins that are known to cluster independently after TCR signaling (Balagopalan et al., 2007). The accumulation of large TCR MCs in the periphery of TSG101 KD continued to engage agonist MHCp (Figure S1E) and resulted in slightly
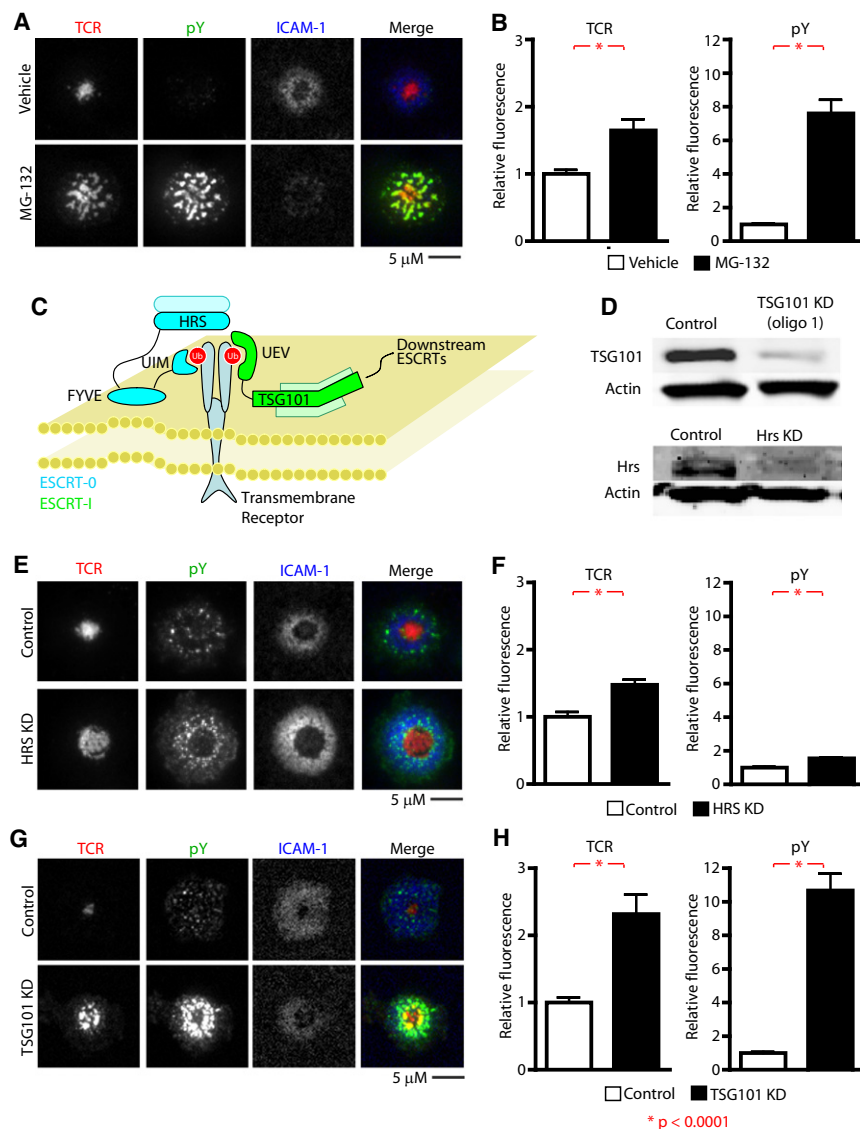
Figure 1. TSG101 Is Required for Central TCR Accumulation and Dephosphorylation

(A and B) AND T cells were pretreated with DMSO (vehicle) or the proteasomal inhibitor MG132 to deplete cells of free ubiquitin. They were then incubated on glass-supported planar bilayers containing 10 molec/μm^2 I-E^k-MCC and 200 molec/μm^2 ICAM-1 for 30 min at 37°C, fixed, and stained for TCR and phosphoytrosine (pY). In (B), bar graphs depict quantification in arbitrary units (AUs) of mean fluorescence at cell contact interfaces and represent >100 cells across three experiments. Standard errors are indicated.

(C) A model for ESCRT recruitment to ubiquitinated substrates. HRS, the critical component of ESCRT-0, binds ubiquitin through its UIM domain but requires recruitment to PI-3-P-rich endosomes through its FYVE domain. TSG101, the critical component of ESCRT-I, binds ubiquitin through its UEV domain.

(D) Cell lysates of 10^6 control TSG101 knockdown (KD) and HRS KD T cells were separated by SDS-PAGE and blotted for TSG101 and HRS. Anti-alpha actin was used as a loading control.

(E and F) Control and HRS KD T cells were incubated on glass-supported planar bilayers containing 10 molec/μm^2 I-E^k-MCC and 200 molec/μm^2 ICAM-1 for 30 min at 37°C, fixed, and stained for TCR and pY. In (F), bar graphs depict quantification in arbitrary units (AU) of mean fluorescence at cell contact interfaces, and represent >100 cells across three experiments. Standard errors are indicated.

(G and H) Control and TSG101 KD T cells were incubated on glass-supported planar bilayers containing 2 molec/μm^2 I-E^k-MCC and 200 molec/μm^2 ICAM-1 for 30 min at 37°C, fixed, and stained for TCR and pY. In (H), bar graphs depict quantification in arbitrary units (AU) of mean fluorescence at cell contact interfaces, and represent >100 cells across three experiments. Standard errors are indicated.

reduced LFA-1-ICAM-1 accumulation in the pSMAC, presumably due to competition with the TCR MCs for space (Figure S1F). The similarity in TCR location and colocalized phosphorylation between the MG132 treatment and TSG101 KD led us to further characterize TSG101's role in IS formation and signal processing.

In order to establish whether TSG101 was positioned to play direct roles in IS patterning, we investigated the distribution of TSG101 within T cells forming ISs. We found that both endogenous and recombinant fluorescent TSG101 were strongly recruited to the cSMAC in response to agonist pMHC engagement on supported planar bilayers (Figure S2).

TSG101 Is Required for cSMAC Formation and Function in T-B Cell Conjugates

It remained possible, although unlikely, that our findings using supported planar bilayers did not faithfully recapitulate IS formation and hence TSG101 function in cell-cell interfaces. To rule out this possibility, we imaged control and TSG101 KD T cells

forming ISs with primary B cells by confocal microscopy. Reconstructed T-B cell interfaces displayed comparable peripheral TCR accumulation and elevated phosphotyrosine after TSG101 KD to those observed on bilayers (Figures 2A–2C). Consistent with our imaging results, flow cytometry analysis of intact or permeabilized T-B cell conjugates demonstrated a significant defect in antigen-induced TCR surface downregulation and degradation, respectively, in the absence of TSG101 (Figure 2D).

We then investigated whether the recruitment of TSG101 to the IS seen in T cells incubated on supported planar bilayers was recapitulated in a cell-cell system. In particular, we wondered whether T cell activation resulted in recruitment of TSG101 to membrane compartments, as would be required in order to execute sorting processes within the IS. We therefore evaluated activation-induced recruitment of TSG101 to T cell membranes by fluorescence resonance energy transfer (FRET) (Wouters et al., 1998). Efficient FRET between membranes and associated signaling proteins has been reported by donor
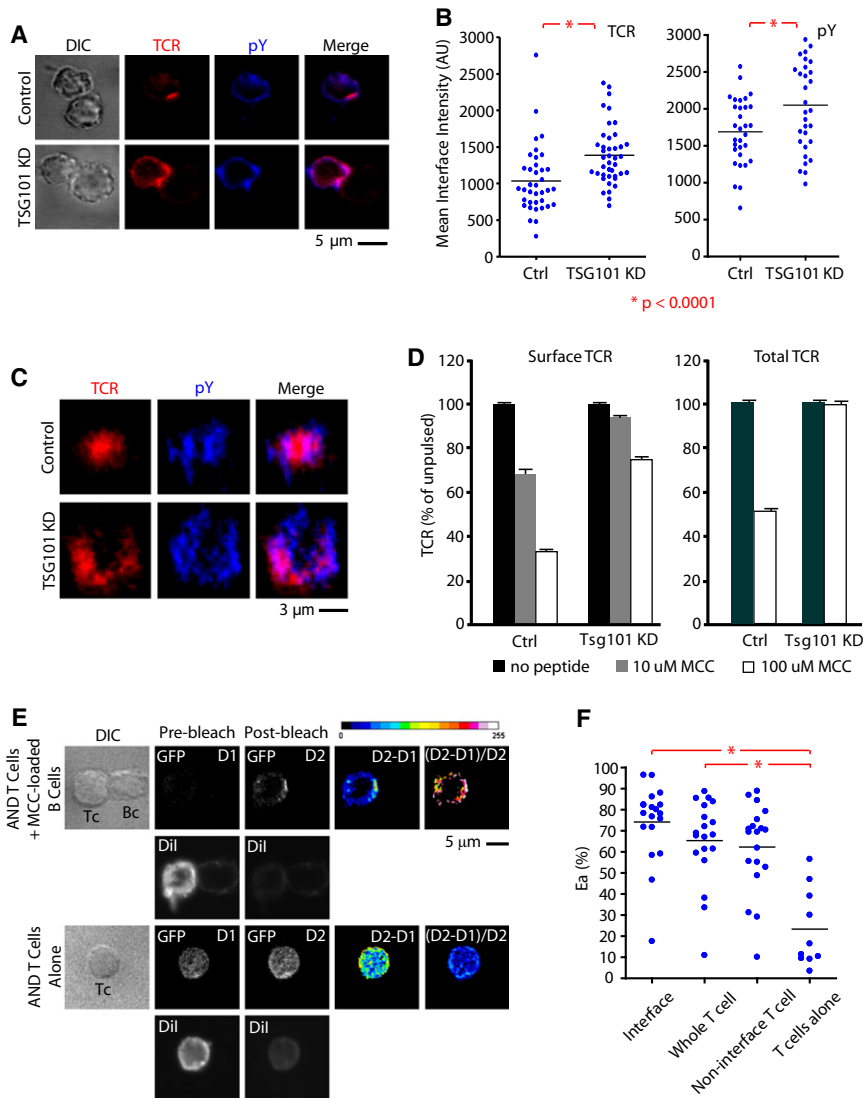
Figure 2. TSG101 Controls Central TCR Accumulation and Dephosphorylation in T Cell-B Cell Conjugates

(A–C) Control and TSG101 KD T cells mixed with MCC-pulsed activated B cells at a 1:2 ratio, and brought into contact by brief centrifugation. After incubation at 37°C for 30 min, cells were fixed, stained for TCR and pY, and placed on clean coverslips for confocal microscopy. Representative (A) images and (B) dot plots demonstrate distribution and quantification of TCR and phosphotyrosine (pY) in Control and TSG101 KD synapses. For en face synapse reconstructions (C), z-stacks of appropriately oriented cell conjugates were collected at 200 nm steps to a distance of ∼8 μm from the coverslip surface.

(D) Control or TSG101 KD T cells were incubated with A20 B cells expressing I-E^k and loaded with either 10 μM or 100 μM MCC. After 30 min, they were cooled to 4°C and either stained directly for surface TCR levels or fixed with 2% PFA, permeabilized with 90% methanol, and stained for total TCR levels with antibodies against the AND TCR Vβ3 region. TCR levels were assessed by flow cytometry. Values are reported as a percent of TCR on T cells in culture with unloaded A20 cells. Standard errors shown are based on 100 cells from two or more experiments.

(E) TSG101-GFP expressing AND T cells were labeled briefly with CM-DiI and incubated either alone or mixed with MCC-pulsed activated B cells at a 1:2 ratio and brought into contact by brief centrifugation. After incubation at 37°C for 30 min, cells were fixed and placed on clean coverslips for confocal microscopy. Cells were imaged for GFP and DiI fluorescence prior to and after photobleaching of DiI (Pre- and Post-bleach). D1 and D2 denote donor (GFP) fluorescence pre- and post-bleach of DiI. D2-D1 is a difference image, and D2-D1/D2 is the FRET image. Both are depicted in pseudo-color (see color key). White represents highest value.

(F) The graph represents apparent FRET (Ea = D2-D1/D2 × 100%) for different regions of the T cell. Lines indicate comparisons, and numbers are p values for comparisons of sample means by ANOVA.

dequenching after acceptor photo-bleaching, with GFP-tagged proteins as donors and the membrane dye DiI as acceptors (McLean et al., 2000). In order to use this method to probe membrane interactions of TSG101, we stably expressed a murine TSG101-GFP chimera in AND T cells by retroviral transduction and sorted them for uniform expression. We then briefly labeled transduced T cells with DiI before allowing them to form conjugates with MCC-loaded murine B cells. Changes in donor fluorescence after photobleaching of DiI revealed a low and diffuse FRET signal throughout the T cell, indicating loose coupling of TSG101 with plasma membrane and endomembranes in the steady state (Figures 2E and 2F) as previously reported (Welsch et al., 2006). Upon IS formation with antigen-pulsed B cells, TSG101 underwent a marked redistribution, polarizing strongly to the IS but also outside the IS (Figures 2E and 2F). The high apparent FRET efficiencies observed is consistent with direct apposition of membranes and tagged TSG101.

Notably, the FRET signal was most prominent at the cSMAC in the T-B cell contacts (Figure 2E). Therefore, T cell activation results in redistribution of TSG101 to membrane compartments concentrated in the IS.

Sorting of TCR MCs into the IS Center Depends on Ub Recognition by TSG101

We then sought to confirm the specificity of TSG101 in inducing cSMAC formation and signal termination. We observed similar defects in cSMAC formation and dephosphorylation when TSG101 was suppressed with three different siRNA oligomers (Figures S3A and S3C). Restoration of wild-type IS patterning by reintroduction of wild-type human TSG101 after KD of endogenous mouse TSG101 indicated that our observed defects in TCR dephosphorylation and cSMAC formation were specifically attributable to TSG101 function (Figures S3A–S3C). However, a mutant TSG101 with substitutions in the UEV domain that
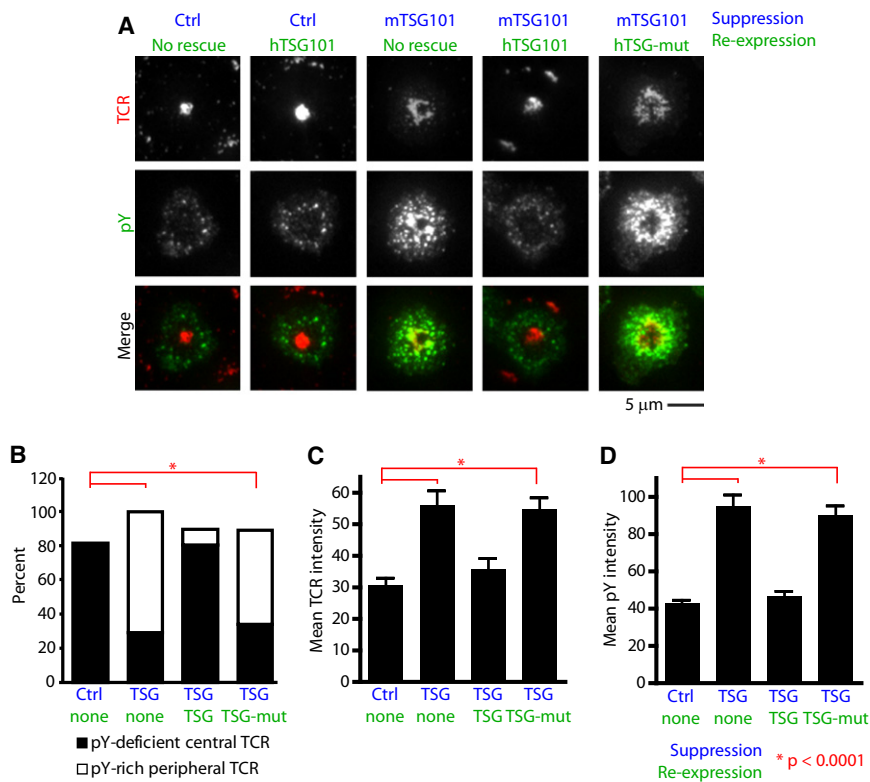
Figure 3. Sorting of TCR into the IS Center Depends on Ubiquitin Recognition by TSG101

Control or TSG101 KD T cells were rescued by infection with retroviral siRNA-resistant constructs containing either wild-type human TSG101 or a construct containing mutations in the UEV domain that abrogates ubiquitin recognition (N45A D46A) (Pornillos et al., 2002). Human TSG101 shares 94.6% amino-acid sequence homology with its murine ortholog.

(A) Shown are T cells transfected with the indicated siRNA (blue) and re-expression vectors forming IS on glass-supported planar bilayers containing 2 molec/μm^2 I-E^k-MCC and 200 molec/μm^2 ICAM-1. Cells were incubated on bilayers for 30 min, fixed, and stained for TCR and pY. Rescue vectors are indicated as wild-type (TSG101) or ubiquitin-binding mutant (TSG-mut).

(B) Synapses were categorized by cSMAC morphology based on central accumulation and phosphotyrosine enrichment.

(C and D) Bar graphs depict quantification in arbitrary units (AU) of mean fluorescence at cell-contact interfaces and represent >100 cells across two or more experiments with standard errors shown.

abrogate Ub binding (Pornillos et al., 2002) was completely unable to restore cSMAC formation or dephosphorylation after TSG101 KD (Figure 3). Cell lysates from TSG101 KD T cells demonstrated a marked accumulation of ubiquitinated species as compared to control siRNA-treated T cells (Figure S3D), and ubiquitination was further increased by agonist MHCp stimulation. These higher-molecular-weight species were also identifiable by antibodies to CD3ζ (Figure S3E). This suggests that CD3ζ may be a ubiquitinated protein recognized by TSG101. In combination with the equivalent defects observed in TSG101 KD and MG132-treated T cells forming ISs, these data support the model that TSG101 specifically interacts with ubiquitinated components of TCR MCs to induce cSMAC formation and TCR signal termination.

Differential Sorting of Receptors by TSG101

Numerous receptors are engaged within the IS that are regulated by diverse mechanisms. A recent example of sorting of such receptors in the IS is the observation that CD28 and TCR traffic together in peripheral MCs upon engagement and are then segregated from each other in the cSMAC (Yokosuka et al., 2008). In light of our finding that Ub-mediated TSG101 recognition is necessary for its incorporation of TCR into a cSMAC, we wondered whether TSG101 might also be involved in segregating TCR from CD28. We evaluated these sorting events by observing control and TSG101 KD T cells interacting with bilayers containing MHCp, ICAM-1, and CD80 and following PKC-θ enriched compartments. Consistent with prior reports, we found that in control cells, PKCθ, and TCRs colocalized in peripheral MCs but became segregated in the cSMAC (Figure 4A and Figure S5A) (Yokosuka et al., 2008). In TSG101

KD T cells, however, PKC-θ and TCR failed to segregate and remained colocalized in large MCs in the pSMAC region, with a significantly elevated Pearson's correlation coefficient (Figure 4A and Figure S4A). Therefore, TSG101 functions at the cSMAC-pSMAC interface to generate distinct TCR- and PKC-θ-enriched domains of the cSMAC.

We then investigated the mechanism by which TSG101 selectively terminates TCR MC signals at the IS center. Normally, TCR MCs become relatively immobile as they accumulate at the IS center (Varma et al., 2006). The association of immobile central TCR with lysobisphosphatidic acid (LBPA) staining is consistent with incorporation of TCR into MVBs (Varma et al., 2006). In control T cells, TCR MCs became immobilized as they became colocalized with LBPA$^+$ structures at the cSMAC (Figures 4B and 4C). In contrast, we observed continued jostling movements of large TCR MCs in the periphery of TSG101 KD IS (Figure 4B and Movie S3). This jostling movement is represented in Figure 4B by overlaying three sequential images at 2 min intervals with red, green, and blue coding such that immobile structures appear white and mobile structures appear colored. The continued jostling of TCR in TSG101 KD IS correlated with a striking segregation of TCR from LBPA$^+$ structures (Figure 4C). This segregation was confirmed by a significant decrease in the Pearson's correlation coefficient between TCR and LBPA in TSG101 KD IS (Figure S4B). Thus, TSG101 is required for TCR colocalization with LBPA$^+$ compartments.

TSG101 Suppression Leads to Chronic TCR Signaling

The striking persistence of phosphorylated TCR MCs after TSG101 KD (Figures 1G and 1H) suggested to us that the duration of signaling through engaged TCR might be extended
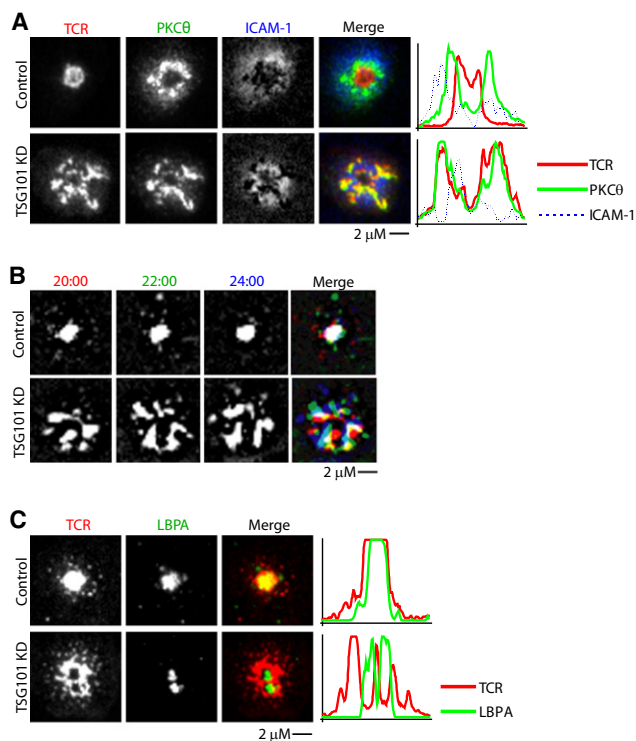
Figure 4. TSG101 Controls Sorting within Plasma Membrane and Endosomal Compartments

(A) Control and TSG101 KD T cells were incubated on glass-supported planar bilayers containing 10 molec/μm^2 I-E^k-MCC, 100 molec/μm^2 CD80, and 200 molec/μm^2 ICAM-1 for 30 min, fixed, and stained for TCR and PKCθ. Images display representative distribution of TCR and PKCθ in control and TSG101 KD synapses.

(B) Control and TSG101 KD T cells were incubated on glass-supported planar bilayers containing 2 molec/μm^2 I-E^k-MCC and 200 molec/μm^2 ICAM-1 and allowed to form contacts for 20 min at 37°C. They were then imaged by TIRFM in the presence of fluorescent anti-TCR Fab. White regions indicate immobilization (overlap of red, green, and blue), whereas any individual color (red green, or blue) indicates movement.

(C) Control and TSG101 KD T cells were incubated on glass-supported planar bilayers containing I-E^k-MCC and ICAM-1 for 30 min at 37°C, fixed, and stained for TCR and LBPA. Images show representative distribution of TCR and LBPA in control and TSG101 KD synapses. All images are representative of >100 cells from at least two experiments.

Figure 5. TSG101 Suppression Leads to Chronic TCR Signaling

(A) Single-cell intracellular calcium measurements were performed on Fura-2 loaded (A) control (n = 91) and (B) TSG101 KD (n = 57) T cells after incubation on glass-supported planar bilayers containing 2 molec/μm^2 I-E^k-MCC and 200 molec/μm^2 ICAM-1 for 10 min at 37°C. Cells were then treated with saturating concentrations (30 μg/mL) of anti-MHC blocking antibodies. Each track depicts individual cell intracellular calcium signal presented as a ratio of fluorescence at 510 nm when excited at 340/380 nm.

(B) Persistent calcium elevation after anti-MHC block was determined as follows: Normally, anti-MHC treatment eliminates elevated Ca^{2+} levels within 2 min. Cells were scored as positive for persistent signaling if intracellular Ca^{2+} levels were 50% above baseline calcium levels for at least 3 min after treatment. Baseline Ca^{2+} values were determined by imaging cells on bilayers containing ICAM-1 alone.

(C) Control and TSG101 KD T cells were loaded with an IL2 capture reagent (Miltenyi) and then incubated on glass-supported planar bilayers containing 2 molec/μm^2 I-E^k-MCC and 200 molec/μm^2 ICAM-1 for 6 hr. Cells were fixed, stained with fluorescent IL2-PE antibodies, and imaged for total PE fluorescence. Bar graphs depict quantification of total IL2 fluorescence per cell in arbitrary units (AUs) and represent >100 cells across three experiments with standard errors.

in TSG101 KD T cells. To test this, we allowed control and TSG101 KD T cells to be activated with agonist MHCp ligand on bilayers for 10 min, sufficient to induce stable TCR engagements, prior to treatment with blocking I-E^k-MCC antibodies (D4) to prevent new TCR MC formation. Signaling was monitored with intracellular Ca^{2+}. In control siRNA-treated T cells, the Ca^{2+} signal decayed over 2 min (Figures 5A and 5B and Figure S5), as previously described (Varma et al., 2006). In contrast, Ca^{2+} elevation decayed only partially and was then sustained at an intermediate level in TSG101 KD T cells after D4 treatment (Figures 5A and 5B and Figure S5). The net effect of increased TCR signaling in TSG101 KD T cells was increased IL-2 production compared to control siRNA-treated T cells (Figure 5C). It was not possible to examine proliferation of T cells in the TSG101 KD because TSG101 is required for the abscission step of cellular
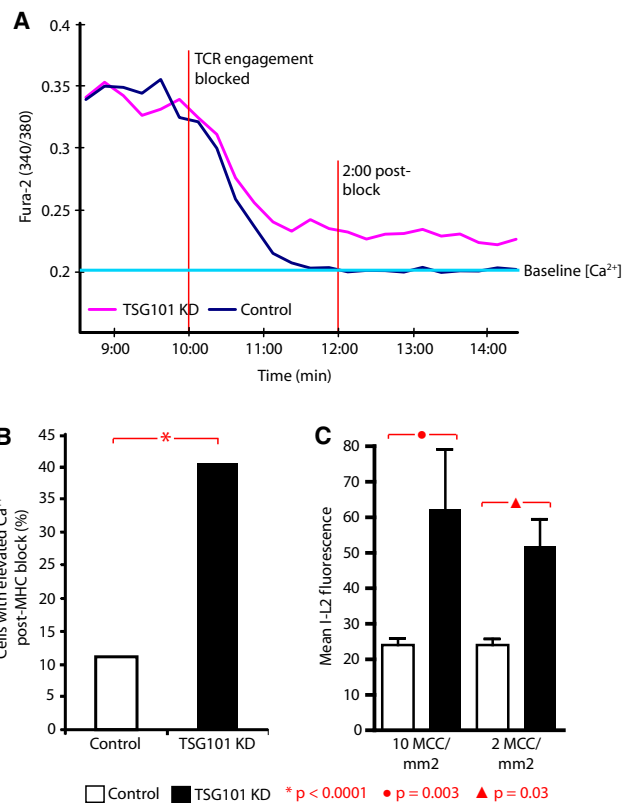
cytokinesis (Morita et al., 2007); as such, we noted that TSG101 KD consistently inhibited T cell proliferation. Thus, TSG101 plays an important role in limiting downstream T cell signals and effector responses after productive proximal signaling in response to TCR engagement.

Weak Agonist MHCp Do Not Involve TSG101

Typical recognition of agonist pMHC results in both tyrosine phosphorylation-mediated T cell activation and Ub-mediated TCR downregulation (Naramura et al., 2002; Samelson et al.,
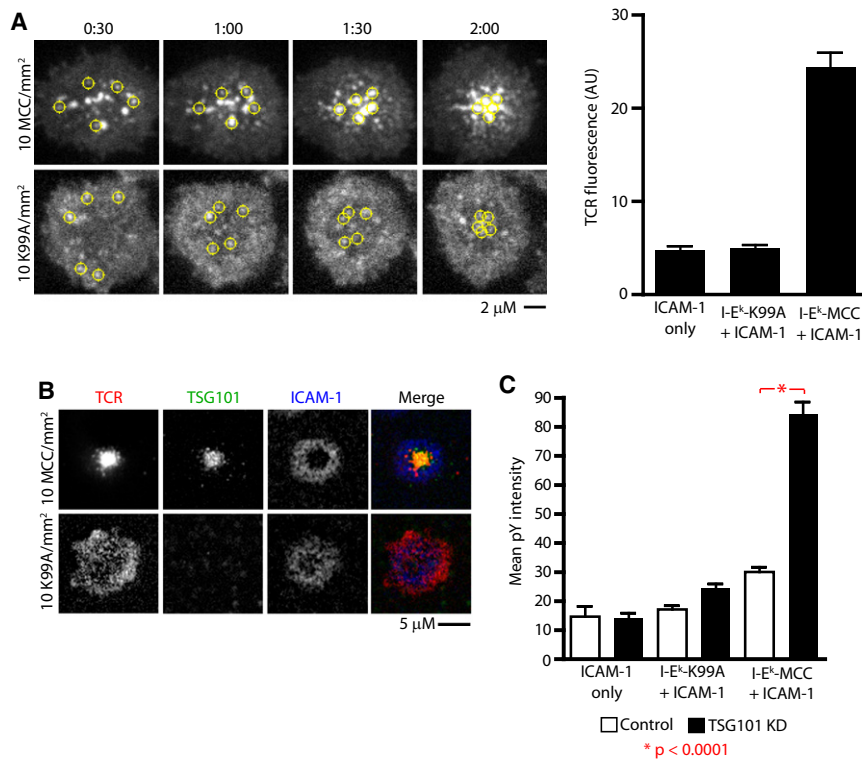
Figure 6. Low-Avidity Ligands Signal through Microclusters but Avoid ESCRT-Mediated TCR Downregulation

(A) AND T cells were incubated on glass-supported planar bilayers containing 200 molec/μm^2 ICAM-1, 100 molec/μm^2 CD80, and 10 molec/μm^2 I-E^k-MCC or I-E^k-K99A as indicated and immediately and imaged by TIRFM at 37°C in the presence of fluorescent anti-TCR Fab. Yellow circles indicate tracks of individual TCR MCs. Bar graph (right) depicts quantification in arbitrary units (AU) of mean TCR fluorescence at cell-contact interfaces in ISs formed by AND T cells in response to ICAM-1, ICAM-1 + I-E^k-K99A, or ICAM-1 + I-E^k-MCC and represent >100 cells across two or more experiments with standard errors.

(B) AND T cells were incubated on glass-supported planar bilayers containing 200 molec/μm^2 ICAM-1, 100 molec/μm^2 CD80, and 10 molec/μm^2 I-E^k-MCC or I-E^k-K99A as indicated for 30 min at 37°C, fixed, and stained for TCR and TSG101. Images show representative distribution of TCR and TSG101 in IS formed in response to I-E^k-MCC or I-E^k-K99A.

(C) Control and TSG101 KD T cells were incubated on glass-supported planar bilayers containing 200 molec/μm^2 ICAM-1, 100 molec/μm^2 CD80, and 10 molec/μm^2 I-E^k-MCC or I-E^k-K99A as indicated for 30 min at 37°C, fixed, and stained for TCR and pY. Bar graphs depict quantification in arbitrary units (AU) of mean pY fluorescence at cell-contact interfaces, and represent >100 cells across two or more experiments with standard errors.

1986). However, T cell activation in the absence of TCR downregulation has recently been reported. The altered peptide ligand (APL) MCC-K99A, a variant of MCC88-103 with a single amino acid substitution that greatly accelerates I-E^k-based tetramer dissociation compared to the native sequence, effectively stimulates proliferation of AND Tg T cells when presented by splenic APCs despite inducing diminished TCR downregulation and central TCR accumulation (Cemerski et al., 2007). We began investigating IS formation by AND T cells in response to I-E^k-MCC-K99A in a planar bilayer system to understand the properties of this ligand-receptor interaction. Supported planar bilayers presenting I-E^k-MCC-K99A and ICAM-1 arrested T cell migration and induced sustained Ca^{2+} elevation in AND T cells only in the presence of CD80 (Figures S6A and S6B). This is consistent with reports in which CD28 engagement is required for response to weak agonist ligands (Bachmann et al., 1997). Real-time imaging of TCR and LFA-1-ICAM-1 interactions demonstrated that, in the presence of CD80, T cells responding to I-E^k-MCC-K99A formed ISs with many structural similarities to I-E^k-MCC-induced ISs. T cells spread symmetrically on K99A-presenting surfaces, and LFA-1-ICAM-1 interactions quickly organized into a pSMAC (Figure S6C). Tyrosine phosphorylation and proximal TCR signaling (indicated by recruitment and phosphorylation of LAT) were concentrated in small MCs in the periphery of the IS with a similar intensity and frequency to IS formed in response to I-E^k-MCC (Figures S6C and S6D). However, in striking contrast to I-E^k-MCC-induced ISs, TCR did not accumulate in the IS center even in response to 10 molecules/μm^2 of I-E^k-MCC-K99A (Figures 6A

and 6B, p < 0.0001; Figures S6C and S6D). Time-lapse TIRFM imaging of IS formed in response to I-E^k-MCC-K99A revealed costimulation dependent formation and centripetal translocation of TCR MCs (Figure 6A and Movie S4); however, these MCs dissipated as they reached the center of the IS rather than accumulating in a cSMAC as they do in response to I-E^k-MCC.

In order to resolve this difference between I-E^k-MCC-K99A and I-E^k-MCC-induced ISs, we investigated the contribution of TSG101 to ISs formed in response to these respective ligands. Notably, TSG101 was recruited to the cSMAC of I-E^k-MCC-induced ISs, but not to I-E^k-MCC-K99A-induced ISs (Figure 6B). Furthermore, TSG101 KD had no impact on TCR MC formation, size, transport, or phosphotyrosine levels within MCC-K99A induced ISs (Figure 6C and Figure S6E). These results demonstrate that TSG101 is not required for early TCR signaling, TCR MC transport, pSMAC formation, or a radially symmetric IS in response to the MCC-K99A weak agonist MHCp. It has previously been demonstrated that TCR MCs form in an F-actin-dependent manner, but then become rapidly F-actin independent on the basis of their stability in the presence of latrunculin A, which sequesters G-actin (Varma et al., 2006). Weak agonist MCC-K99A-induced TCR MCs remained F-actin dependent, in contrast to many F-actin-independent MCs that accumulation in response to I-E^k-MCC (Figure S6F). The cSMAC is generally free or depleted of F-actin (Kaizuka et al., 2007). Analysis of the F-actin distribution in the IS formed in response to MCC and MCC-K99A MHCp confirmed that I-E^k-MCC-K99A does not induce an F-actin-free central zone (Figure S6G).

DISCUSSION

We previously demonstrated that the cSMAC shows a striking enrichment of LBPA (Varma et al., 2006), a lipid associated with MVBs. This suggested that the cSMAC might be a site for degradation of TCR through an ESCRT-dependent pathway (Williams and Urbé, 2007). Other results in the field were consistent with this notion including earlier observations that CD2AP, an adaptor linking actin and Cbl family ubiquitin E3-ligases is required for normal TCR degradation and signal termination in the cSMAC (Lee et al., 2003). There was also ample evidence for a role of Cbl family E3 ligases in TCR signal termination and a role for lysosomes in TCR degradation (Liu et al., 2000; Naramura et al., 2002; Valitutti et al., 1997). It had also been demonstrated that TCR downregulation correlates with MHCp potency (Itoh et al., 1999) and that a subset of weak agonist ligands do not trigger TCR downregulation at all (Cemerski et al., 2007). Furthermore, the TCR ζ and δ chains are directly ubiquitinated upon strong TCR engagement (Cenciarelli et al., 1992). On the basis of these observations, we anticipated that ubiquitination and ESCRT machinery might be important for TCR signal termination and eventual degradation after engagement with agonist MHCp. We were surprised by our finding in this study that depletion of free ubiquitin with MG132 or knockdown of TSG101 not only blocked TCR signal termination and degradation but also blocked cSMAC formation in response to agonist MHCp. In contrast, a weak agonist MHCp could induce robust TCR MCs, Ca^{2+} elevation, and pSMAC formation without recruiting TSG101 or inducing a cSMAC in normal T cells. These results have important implications for signal integration in response to agonist MHCp and how this differs from weak agonist MHCp.

Our results suggest distinct roles for major Ub-recognizing ESCRT components HRS and TSG101 in IS formation and TCR downregulation. HRS is part of ESCRT-0 and associates with ubiquitinated cargo through its ubiquitin interaction motif (UIM) (Bache et al., 2003b; Hirano et al., 2006), in parallel with inositol-3-phosphate-bearing lipids present in endosomes (Raiborg et al., 2001). In EGFR systems, HRS promotes ubiquitin recognition by TSG101 by directing TSG101 to early endosomes containing ubiquitinated cargo (Katzmann et al., 2003). This process is dependent on the recruitment of HRS recruitment to receptors within clathrin lattices (Raiborg et al., 2002), and clathrin clustering of ubiquitinated cargo is required for efficient HRS recognition (Raiborg et al., 2006). Indeed, in EGF-R systems involving both clathrin-dependent and clathrin-independent endocytic mechanisms, HRS is involved only in degradation of clathrin-endocytosed receptors (Myromslien et al., 2006). The specificity of HRS for clathrin-coated pits and the failure of TCR MCs to intersect with these compartments may explain the finding that a cSMAC is formed in the absence of HRS (Razi and Futter, 2006). Furthermore, in non-EGFR systems, the association of HRS and TSG101 is not so clear. Indeed, TSG101-mediated endosomal trafficking of Tyrp1 is independent of HRS function in melanocytes (Truschel et al., 2009). Furthermore, HRS is involved in alternate internal trafficking pathways, such as sequence-dependent recycling of the beta-2 adrenergic receptor (Hanyaloglu et al., 2005). Thus, prior models suggesting a strictly sequential transfer of ubiquitinated cargo from ESCRT-0 to ESCRT-I may not apply in all situations, as has been recently demonstrated (Shields et al., 2009). Downregulation of engaged TCR complexes appears to be clathrin independent (Monjas et al., 2004), whereas internalization of the proximal signaling molecule LAT has been shown to be clathrin dependent (Brignatz et al., 2005). We detected a weak but significant effect of HRS KD on non-TCR MC-associated phosphotyrosine. This suggests that HRS may act on distinct substrates from the TCR during T cell activation and this is worthy of further study.

Our results provide insight into the distinct mechanisms of sustained signaling by agonist and weak agonist MHCp. TSG101 prevents chronic signaling by agonist MHCp induced TCR MCs. TCR-agonist MHCp and CD28-CD80 interactions are initially colocalized in MCs, but then are segregated within the cSMAC (Yokosuka et al., 2008). We show that this segregation requires TSG101. There are a number of possibilities for how TSG101 organizes this process. Two possibilities are polymerization of ESCRT III components to generate MVBs that are then translocated toward the center by microtubules (Wollert et al., 2009) or linkage to a final actin-dependent translocation step through Alix before later ESCRT steps are initiated (Pan et al., 2006; Strack et al., 2003). This sorting process, however mediated, led to formation of the PKC-θ-rich compartment, which is a hallmark of the IS formed with professional APCs (Monks et al., 1997; Tseng et al., 2008; Yokosuka et al., 2008). Weak against MHCp required CD80 in the bilayer to form TCR MCs and sustain Ca^{2+} signals, which is not the case for agonist MHCp. This result is consistent with earlier studies showing that responses to weak against MHCp are CD28 dependent (Bachmann et al., 1997). Weak agonist MCC-K99A induced TCR MCs that remained F-actin dependent and disappeared in the center of the IS without a requirement for an F-actin free central zone or TSG101. The mechanism by which weak agonist MHCp signals are terminated is not clear, but we speculate that the requirement for a dynamic contribution from CD80 and the continued requirement for F-actin may enable physical disengagement and recycling of TCR at the point of convergence of centripetal F-actin flow (Kaizuka et al., 2007). More stable MCs formed by agonist MHCp might persist in response to the same physical process, necessitating the use of TSG101 to mark irreversibly clustered TCR-MHCp complex for elimination. The other distinguishing feature of signaling mediated by agonist and weak agonist MHCp is the generation of the consolidated PKC-θ-rich compartment by agonist MHCp. Given that the cSMAC size is linearly related to agonist MHCp density (Varma et al., 2006), the formation of the PKC-θ-rich outer cSMAC may provide a mechanism to measure integrated TCR avidity in an IS as long as CD80 or CD86 are present on the APC.

These data lead us to a model in which ESCRT-I is required for sorting of TCR into MVB-like structures within the cSMAC and for signal termination in response to agonist MHCp. TCR and CD28 engagements occur primarily in the IS dSMAC, resulting in receptor phosphorylation, actin-driven centripetal movement of microclusters, and ubiquitination of TCRs but not CD28 complexes. Upon reaching the border between the pSMAC and cSMAC, TSG101 specifically sorts strong agonist-engaged ubiquitinated TCR into central MVB or lysosomal compartments, leaving CD28 along with associated PKCθ to accumulate and

continue signaling from an annular cluster. Weak agonist-engaged TCR clusters are not subject to TSG101-mediated sorting and are thus not incorporated into the cSMAC. Our findings clarify the mechanism of cSMAC formation and the origin of recently described segregation of inner TCR and outer, PKC-θ-enriched, cSMAC regions (Kaizuka et al., 2007; Varma et al., 2006; Yokosuka et al., 2008). Integrating TSG101 into our current picture of IS structure clarifies the inhibitory role of the cSMAC and the sorting function of TSG101 reconciles the coexistence of signaling and degradation compartments within this central structure in T cell activation (Cemerski et al., 2008; Lee et al., 2003; Varma et al., 2006).

SUPPLEMENTAL INFORMATION

Supplemental Information includes six figures, four movies, and Supplemental Experimental Procedures and can be found with this article online at doi:10.1016/j.immuni.2010.04.005.

REFERENCES

Bache, K.G., Brech, A., Mehlum, A., and Stenmark, H. (2003a). Hrs regulates multivesicular body formation via ESCRT recruitment to endosomes. J. Cell Biol. 162, 435–442.

Bache, K.G., Raiborg, C., Mehlum, A., and Stenmark, H. (2003b). STAM and Hrs are subunits of a multivalent ubiquitin-binding complex on early endosomes. J. Biol. Chem. 278, 12513–12521.

Bache, K.G., Stuffers, S., Malerød, L., Slagsvold, T., Raiborg, C., Lechardeur, D., Wälchli, S., Lukacs, G.L., Brech, A., and Stenmark, H. (2006). The ESCRT-III subunit hVps24 is required for degradation but not silencing of the epidermal growth factor receptor. Mol. Biol. Cell 17, 2513–2523.

Bachmann, M.F., McKall-Faienza, K., Schmits, R., Bouchard, D., Beach, J., Speiser, D.E., Mak, T.W., and Ohashi, P.S. (1997). Distinct roles for LFA-1 and CD28 during activation of naive T cells: Adhesion versus costimulation. Immunity 7, 549–557.

Balagopalan, L., Barr, V.A., Sommers, C.L., Barda-Saad, M., Goyal, A., Isakowitz, M.S., and Samelson, L.E. (2007). c-Cbl-mediated regulation of LAT-nucleated signaling complexes. Mol. Cell. Biol. 27, 8622–8636.

Bilodeau, P.S., Winistorfer, S.C., Kearney, W.R., Robertson, A.D., and Piper, R.C. (2003). Vps27-Hse1 and ESCRT-I complexes cooperate to increase efficiency of sorting ubiquitinated proteins at the endosome. J. Cell Biol. 163, 237–243.

Brignatz, C., Restouin, A., Bonello, G., Olive, D., and Collette, Y. (2005). Evidences for ubiquitination and intracellular trafficking of LAT, the linker of activated T cells. Biochim. Biophys. Acta 1746, 108–115.

Bunnell, S.C., Hong, D.I., Kardon, J.R., Yamazaki, T., McGlade, C.J., Barr, V.A., and Samelson, L.E. (2002). T cell receptor ligation induces the formation of dynamically regulated signaling assemblies. J. Cell Biol. 158, 1263–1275.

Campi, G., Varma, R., and Dustin, M.L. (2005). Actin and agonist MHC-peptide complex-dependent T cell receptor microclusters as scaffolds for signaling. J. Exp. Med. 202, 1031–1036.

Cemerski, S., Das, J., Locasale, J., Arnold, P., Giurisato, E., Markiewicz, M.A., Fremont, D., Allen, P.M., Chakraborty, A.K., and Shaw, A.S. (2007). The stimulatory potency of T cell antigens is influenced by the formation of the immunological synapse. Immunity 26, 345–355.

Cemerski, S., Das, J., Giurisato, E., Markiewicz, M.A., Allen, P.M., Chakraborty, A.K., and Shaw, A.S. (2008). The balance between T cell receptor signaling and degradation at the center of the immunological synapse is determined by antigen quality. Immunity 29, 414–422.

Cenciarelli, C., Hou, D., Hsu, K.C., Rellahan, B.L., Wiest, D.L., Smith, H.T., Fried, V.A., and Weissman, A.M. (1992). Activation-induced ubiquitination of the T cell antigen receptor. Science 257, 795–797.

Davis, M.M., Krogsgaard, M., Huse, M., Huppa, J., Lillemeier, B.F., and Li, Q.J. (2007). T cells as a self-referential, sensory organ. Annu. Rev. Immunol. 25, 681–695.

Doyotte, A., Russell, M.R., Hopkins, C.R., and Woodman, P.G. (2005). Depletion of TSG101 forms a mammalian "Class E" compartment: A multicis-ternal early endosome with multiple sorting defects. J. Cell Sci. 118, 3003–3017.

Dustin, M.L. (2002). The immunological synapse. Arthritis Res. 4 (Suppl 3), S119–S125.

Dustin, M.L. (2008). T-cell activation through immunological synapses and kinapses. Immunol. Rev. 221, 77–89.

Dustin, M.L., Olszowy, M.W., Holdorf, A.D., Li, J., Bromley, S., Desai, N., Widder, P., Rosenberger, F., van der Merwe, P.A., Allen, P.M., and Shaw, A.S. (1998). A novel adaptor protein orchestrates receptor patterning and cytoskeletal polarity in T-cell contacts. Cell 94, 667–677.

Grakoui, A., Bromley, S.K., Sumen, C., Davis, M.M., Shaw, A.S., Allen, P.M., and Dustin, M.L. (1999). The immunological synapse: A molecular machine controlling T cell activation. Science 285, 221–227.

Hanyaloglu, A.C., McCullagh, E., and von Zastrow, M. (2005). Essential role of Hrs in a recycling mechanism mediating functional resensitization of cell signaling. EMBO J. 24, 2265–2283.

Hirano, S., Kawasaki, M., Ura, H., Kato, R., Raiborg, C., Stenmark, H., and Wakatsuki, S. (2006). Double-sided ubiquitin binding of Hrs-UIM in endosomal protein sorting. Nat. Struct. Mol. Biol. 13, 272–277.

Huang, J., Lo, P.F., Zal, T., Gascoigne, N.R., Smith, B.A., Levin, S.D., and Grey, H.M. (2002). CD28 plays a critical role in the segregation of PKC theta within the immunologic synapse. Proc. Natl. Acad. Sci. USA 99, 9369–9373.

Huppa, J.B., and Davis, M.M. (2003). T-cell-antigen recognition and the immunological synapse. Nat. Rev. Immunol. 3, 973–983.

Huse, M., Klein, L.O., Girvin, A.T., Faraj, J.M., Li, Q.J., Kuhns, M.S., and Davis, M.M. (2007). Spatial and temporal dynamics of T cell receptor signaling with a photoactivatable agonist. Immunity 27, 76–88.

Isakov, N., and Altman, A. (2002). Protein kinase C(theta) in T cell activation. Annu. Rev. Immunol. 20, 761–794.

Itoh, Y., Hemmer, B., Martin, R., and Germain, R.N. (1999). Serial TCR engagement and down-modulation by peptide:MHC molecule ligands: Relationship to the quality of individual TCR signaling events. J. Immunol. 162, 2073–2080.

Kaizuka, Y., Douglass, A.D., Varma, R., Dustin, M.L., and Vale, R.D. (2007). Mechanisms for segregating T cell receptor and adhesion molecules during immunological synapse formation in Jurkat T cells. Proc. Natl. Acad. Sci. USA 104, 20296–20301.

Katzmann, D.J., Stefan, C.J., Babst, M., and Emr, S.D. (2003). Vps27 recruits ESCRT machinery to endosomes during MVB sorting. J. Cell Biol. 162, 413–423.

Krogsgaard, M., Huppa, J.B., Purbhoo, M.A., and Davis, M.M. (2003). Linking molecular and cellular events in T-cell activation and synapse formation. Semin. Immunol. 15, 307–315.

Krummel, M.F., Sjaastad, M.D., Wülfing, C., and Davis, M.M. (2000). Differential clustering of CD4 and CD3zeta during T cell recognition. Science 289, 1349–1352.

Lee, K.H., Dinner, A.R., Tu, C., Campi, G., Raychaudhuri, S., Varma, R., Sims, T.N., Burack, W.R., Wu, H., Wang, J., et al. (2003). The immunological synapse balances T cell receptor signaling and degradation. Science 302, 1218–1222.

Liu, H., Rhodes, M., Wiest, D.L., and Vignali, D.A. (2000). On the dynamics of TCR:CD3 complex cell surface expression and downmodulation. Immunity *13*, 665–675.

McLean, P.J., Kawamata, H., Ribich, S., and Hyman, B.T. (2000). Membrane association and protein conformation of alpha-synuclein in intact neurons. Effect of Parkinson's disease-linked mutations. J. Biol. Chem. *275*, 8812–8816.

Melikova, M.S., Kondratov, K.A., and Kornilova, E.S. (2006). Two different stages of epidermal growth factor (EGF) receptor endocytosis are sensitive to free ubiquitin depletion produced by proteasome inhibitor MG132. Cell Biol. Int. *30*, 31–43.

Monjas, A., Alcover, A., and Alarcón, B. (2004). Engaged and bystander T cell receptors are down-modulated by different endocytotic pathways. J. Biol. Chem. *279*, 55376–55384.

Monks, C.R., Kupfer, H., Tamir, I., Barlow, A., and Kupfer, A. (1997). Selective modulation of protein kinase C-theta during T-cell activation. Nature *385*, 83–86.

Monks, C.R., Freiberg, B.A., Kupfer, H., Sciaky, N., and Kupfer, A. (1998). Three-dimensional segregation of supramolecular activation clusters in T cells. Nature *395*, 82–86.

Morita, E., Sandrin, V., Chung, H.Y., Morham, S.G., Gygi, S.P., Rodesch, C.K., and Sundquist, W.I. (2007). Human ESCRT and ALIX proteins interact with proteins of the midbody and function in cytokinesis. EMBO J. *26*, 4215–4227.

Myromslien, F.D., Grøvdal, L.M., Raiborg, C., Stenmark, H., Madshus, I.H., and Stang, E. (2006). Both clathrin-positive and -negative coats are involved in endosomal sorting of the EGF receptor. Exp. Cell Res. *312*, 3036–3048.

Naramura, M., Jang, I.K., Kole, H., Huang, F., Haines, D., and Gu, H. (2002). c-Cbl and Cbl-b regulate T cell responsiveness by promoting ligand-induced TCR down-modulation. Nat. Immunol. *3*, 1192–1199.

Pan, S., Wang, R., Zhou, X., He, G., Koomen, J., Kobayashi, R., Sun, L., Corvera, J., Gallick, G.E., and Kuang, J. (2006). Involvement of the conserved adaptor protein Alix in actin cytoskeleton assembly. J. Biol. Chem. *281*, 34640–34650.

Pornillos, O., Alam, S.L., Rich, R.L., Myszka, D.G., Davis, D.R., and Sundquist, W.I. (2002). Structure and functional interactions of the Tsg101 UEV domain. EMBO J. *21*, 2397–2406.

Raiborg, C., Bremnes, B., Mehlum, A., Gillooly, D.J., D'Arrigo, A., Stang, E., and Stenmark, H. (2001). FYVE and coiled-coil domains determine the specific localisation of Hrs to early endosomes. J. Cell Sci. *114*, 2255–2263.

Raiborg, C., Bache, K.G., Gillooly, D.J., Madshus, I.H., Stang, E., and Stenmark, H. (2002). Hrs sorts ubiquitinated proteins into clathrin-coated microdomains of early endosomes. Nat. Cell Biol. *4*, 394–398.

Raiborg, C., Wesche, J., Malerød, L., and Stenmark, H. (2006). Flat clathrin coats on endosomes mediate degradative protein sorting by scaffolding Hrs in dynamic microdomains. J. Cell Sci. *119*, 2414–2424.

Razi, M., and Futter, C.E. (2006). Distinct roles for Tsg101 and Hrs in multive-sicular body formation and inward vesiculation. Mol. Biol. Cell *17*, 3469–3483.

Samelson, L.E., Patel, M.D., Weissman, A.M., Harford, J.B., and Klausner, R.D. (1986). Antigen activation of murine T cells induces tyrosine phosphory-lation of a polypeptide associated with the T cell antigen receptor. Cell *46*, 1083–1090.

Shields, S.B., Oestreich, A.J., Winistorfer, S., Nguyen, D., Payne, J.A., Katzmann, D.J., and Piper, R. (2009). ESCRT ubiquitin-binding domains function cooperatively during MVB cargo sorting. J. Cell Biol. *185*, 213–224.

Sims, T.N., Soos, T.J., Xenias, H.S., Dubin-Thaler, B., Hofman, J.M., Waite, J.C., Cameron, T.O., Thomas, V.K., Varma, R., Wiggins, C.H., et al. (2007). Opposing effects of PKCtheta and WASp on symmetry breaking and reloca-tion of the immunological synapse. Cell *129*, 773–785.

Strack, B., Calistri, A., Craig, S., Popova, E., and Göttlinger, H.G. (2003). AIP1/ALIX is a binding partner for HIV-1 p6 and EIAV p9 functioning in virus budding. Cell *114*, 689–699.

Sun, Z., Arendt, C.W., Ellmeier, W., Schaeffer, E.M., Sunshine, M.J., Gandhi, L., Annes, J., Petrzilka, D., Kupfer, A., Schwartzberg, P.L., and Littman, D.R. (2000). PKC-theta is required for TCR-induced NF-kappaB activation in mature but not immature T lymphocytes. Nature *404*, 402–407.

Sundquist, W.I., Schubert, H.L., Kelly, B.N., Hill, G.C., Holton, J.M., and Hill, C.P. (2004). Ubiquitin recognition by the human TSG101 protein. Mol. Cell *13*, 783–789.

Teo, H., Veprintsev, D.B., and Williams, R.L. (2004). Structural insights into endosomal sorting complex required for transport (ESCRT-I) recognition of ubiquitinated proteins. J. Biol. Chem. *279*, 28689–28696.

Truschel, S.T., Simoes, S., Setty, S.R., Harper, D.C., Tenza, D., Thomas, P.C., Herman, K.E., Sackett, S.D., Cowan, D.C., Theos, A.C., et al. (2009). ESCRT-I function is required for Tyrp1 transport from early endosomes to the melano-some limiting membrane. Traffic *10*, 1318–1336.

Tseng, S.Y., Waite, J.C., Liu, M., Vardhana, S., and Dustin, M.L. (2008). T cell-dendritic cell immunological synapses contain TCR-dependent CD28-CD80 clusters that recruit protein kinase C theta. J. Immunol. *181*, 4852–4863.

Valitutti, S., Müller, S., Salio, M., and Lanzavecchia, A. (1997). Degradation of T cell receptor (TCR)-CD3-zeta complexes after antigenic stimulation. J. Exp. Med. *185*, 1859–1864.

Varma, R., Campi, G., Yokosuka, T., Saito, T., and Dustin, M.L. (2006). T cell receptor-proximal signals are sustained in peripheral microclusters and terminated in the central supramolecular activation cluster. Immunity *25*, 117–127.

Welsch, S., Habermann, A., Jäger, S., Müller, B., Krijnse-Locker, J., and Kräusslich, H.G. (2006). Ultrastructural analysis of ESCRT proteins suggests a role for endosome-associated tubular-vesicular membranes in ESCRT function. Traffic *7*, 1551–1566.

Williams, R.L., and Urbé, S. (2007). The emerging shape of the ESCRT machinery. Nat. Rev. Mol. Cell Biol. *8*, 355–368.

Wollert, T., Wunder, C., Lippincott-Schwartz, J., and Hurley, J.H. (2009). Membrane scission by the ESCRT-III complex. Nature *458*, 172–177.

Wouters, F.S., Bastiaens, P.I., Wirtz, K.W., and Jovin, T.M. (1998). FRET microscopy demonstrates molecular association of non-specific lipid transfer protein (nsL-TP) with fatty acid oxidation enzymes in peroxisomes. EMBO J. *17*, 7179–7189.

Yokosuka, T., Sakata-Sogawa, K., Kobayashi, W., Hiroshima, M., Hashimoto-Tane, A., Tokunaga, M., Dustin, M.L., and Saito, T. (2005). Newly generated T cell receptor microclusters initiate and sustain T cell activation by recruitment of Zap70 and SLP-76. Nat. Immunol. *6*, 1253–1262.

Yokosuka, T., Kobayashi, W., Sakata-Sogawa, K., Takamatsu, M., Hashimoto-Tane, A., Dustin, M.L., Tokunaga, M., and Saito, T. (2008). Spatiotemporal regulation of T cell costimulation by TCR-CD28 microclusters and protein kinase C theta translocation. Immunity *29*, 589–601.